Eur. Phys. J. A **14**, 365–370 (2002)
DOI 10.1140/epja/i2002-10013-1

THE EUROPEAN PHYSICAL JOURNAL A

Yields of neutron-rich isotopes around $Z = 28$ produced in 30 MeV proton-induced fission of ^{238}U

K. Kruglov[1,a], A. Andreyev[2], B. Bruyneel[1], S. Dean[1], S. Franchoo[3], M. Górska[4], K. Helariutta[4], M. Huyse[1], Yu. Kudryavtsev[1], W.F. Mueller[5], N.V.S.V. Prasad[1], R. Raabe[6], K.-H. Schmidt[4,b], P. Van Duppen[1], J. Van Roosbroeck[1], K. Van de Vel[1], and L. Weissman[5]

[1] Instituut voor Kern- en Stralingsfysica, University of Leuven, Celestijnenlaan 220D, B-3001 Leuven, Belgium
[2] University of Liverpool, UK
[3] CERN-ISOLDE, Switzerland
[4] GSI, D-64291, Darmstadt, Germany
[5] MSU, East Lansing, MI, USA
[6] CEA, Saclay, France

Received: 11 February 2002 / Revised version: 25 April 2002
Communicated by J. Äystö

Abstract. Heavy $^{65\text{-}70}$Co, $^{68\text{-}74}$Ni, $^{70\text{-}76}$Cu and $^{74\text{-}81}$Ga isotopes were produced at the LISOL facility by means of 30 MeV proton-induced fission of ^{238}U. Production rates were deduced and compared to two types of cross-section calculations: the empirical model (V. Rubchenya, private communication) and the PROFI code. Comparison with experimental data favors the latter model. Yields using different beam-target combinations and different energies are calculated and discussed.

PACS. 24.10.-i Nuclear-reaction models and methods – 24.75.+i General properties of fission – 25.85.Ge Charged-particle-induced fission – 29.25.Rm Sources of radioactive nuclei

1 Introduction

The study of the doubly magic nucleus ^{78}Ni ($Z = 28$ and $N = 50$) and the nuclei in its neighborhood is a challenge from the experimental as well as from the theoretical point of view. The data can form a stringent test for different theoretical models and can improve our understanding of the nuclei and the interactions between the nucleons [1]. Moreover, the properties of the exotic nuclei around the proton number $Z = 28$ and the neutron number $N = 50$ might influence the r-process and in this way affect the stellar nucleosynthesis.

Due to the current experimental limitations the data on these nuclei are scarce; the ^{78}Ni has recently been identified at GSI using relativistic fission but no further information on its properties is available [2]. Nuclei in the neighborhood of ^{78}Ni have been produced using different methods:

- high-energy (600 to 1000 MeV) proton-induced fission of ^{238}U followed by thermochromatographic techniques and on-line mass separation [3] at the ISOLDE on-line isotope separator;
- thermal neutron-induced fission of ^{235}U followed by thermochromatographic techniques and mass separation at the OSIRIS facility [4];
- thermal neutron-induced fission of ^{235}U followed by in-flight separation at the Lohengrin spectrometer [5];
- low-energy (25 to 30 MeV) proton-induced fission of ^{238}U followed by thermalisation in a gas catcher and on-line mass separation [6,7]. In this case resonant laser ionization has been applied to improve the selectivity [6];
- intermediate-energy fragmentation of heavy-ion beams followed by in-flight fragment separation [8–10];
- relativistic energy fission of ^{238}U on a ^{9}Be target followed by in-flight fragment separation [2].

The production rates for all methods depend on the cross-section of the produced nuclei and the luminosity of the beam-target system. Of course, the separation technique plays also a crucial role in the whole process. For example beams of elements like cobalt ($Z = 27$) and iron ($Z = 26$) are difficult to produce with the standard high-temperature target techniques used for example at ISOLDE because of the relatively long delay times for these elements.

In this paper we concentrate on the cross-section of the low-energy proton-induced fission of ^{238}U. Isotopic

[a] e-mail: Kirill.krouglov@fys.kuleuven.ac.be
[b] e-mail: K.h.schmidt@gsi.de

cross-section values for these nuclei far from stability produced in this reaction are in general poorly known and theoretical descriptions used to extrapolate measured cross-sections and/or production rates towards these unknown regions often fail. Furthermore, reliable experimental cross-section data are seldom available.

Two major techniques are used to measure the cross-sections: in-flight and on-line isotope separation. In the first method, the separation efficiency can be determined rather precisely. The last method is based on radioactive decay measurements after mass separation and suffers from a number of experimental difficulties. These are related to the instability of the ion-source efficiency and its dependence on the chemical properties of the studied element. Additionally, absolute intensities of γ-rays are not always known. Finally, if only mass separation is applied without Z selection, cumulative effects of isobaric decays have to be disentangled. In our method (selective laser ionization applied) we do not suffer from such effect.

Recently, a new cross-section calculation was performed and compared with experimental data obtained at the IGISOL facility [7]. From these calculations a cross-section for ^{78}Ni of 2.8 nb was extrapolated [11]. At the LISOL facility [12] we have developed a new type of ion source based on thermalisation of reaction products in a buffer-gas cell followed by resonant photo-ionization by laser light. Thanks to its element selectivity, this development allows detailed β-decay spectroscopy of neutron-rich nickel and cobalt isotopes [6,13] and a measurement of the isotopic yields of weakly produced fission products in a reliable way and with a reasonable degree of accuracy.

In this paper we report on isotopic fission yields for cobalt, nickel, copper and gallium from 30 MeV proton-induced fission of ^{238}U. We compare the data with calculations performed within the PROFI code [14,15] and within the model of [11]. A strong discrepancy between the two predictions exists, and our data favor the model of Benlliure *et al.* [14,15]. Based on the latter, an estimate for the cross-section of ^{78}Ni is deduced and the influence of the beam energy and of beam-target combination is discussed.

In the next section we will discuss the experimental procedure to obtain the production rates. In the subsequent section the obtained results are compared with model predictions, and the influence of the different experimental parameters is investigated.

2 Experimental setup and results

The neutron-rich isotopes are produced in a 30 MeV proton-induced fission reaction of ^{238}U. Two ^{238}U targets (10 mg/cm^2) are situated in a gas cell. The targets are tilted under an angle of 20° with respect to the proton beam (3 μA) [12]. The fission products are thermalized and neutralized in 500 mbar argon gas, laser ionized using a two-step resonant ionization process and transported with the flow of the argon gas through the exit hole of the gas cell. The available laser power was enough to saturate the laser ionization schemes used for the three different elements (Co, Ni and Cu). In this way the laser ionization process as such had an efficiency close to 100%. Subsequently, the ions are guided by a radiofrequency sextupole ion guide to the extraction electrode and analyzing magnet. After mass separation, the ions are implanted onto a tape situated in front of a detection setup consisting of two high-volume (70% and 75%) germanium-detectors for gamma detection and thin plastic ΔE-detectors for β-detection. The activity was implanted in a cycle mode with beam-on and -off periods adapted to the isotope's half-life. The tape could be moved after every cycle in order to reduce the build-up of daughter radioactivity. Two types of data were collected in parallel: singles multispectra data and coincidence data in event-by-event mode. For the last mode any of the γ-γ or β-γ coincidence conditions was used as a trigger to record an event. Every good event obtained a time stamp from a time-to-digital converter that marked the time difference between the start of the implantation cycle and the detection of the event. Absolute γ-ray efficiencies were calculated using GEANT simulations [16] while β-detection efficiencies were obtained by comparing singles gamma spectra with β-gated spectra. Because of the laser ionization process the contribution from non-resonantly produced ions —*i.e.* ions that do not neutralize during thermalization and transportation through the exit hole— could be easily evaluated be measuring production rates with the lasers off. It also allowed, in some cases where absolute γ-ray intensities were not known, to deduce them from known absolute γ-ray intensities from daughter products.

The production rates of $^{67\text{-}70}$Co and $^{68\text{-}74}$Ni isotopes are known from earlier studies at LISOL [13]. Recently, yields were deduced for the $^{65\text{-}66}$Co, $^{70\text{-}76}$Cu isotopes, produced with resonant laser ionization, and $^{74\text{-}81}$Ga without laser ionization, since a significant fraction of the Ga isotopes survives the neutralization process. This could be explained by the fact that Ga-atoms have a lower ionization potential than Ni (6.0 eV (Ga) *vs.* 7.6 eV (Ni)), thus having a higher probability to be ionized by plasma or by the collisions with impurity molecules or metastable Ar-atoms.

In order to verify the consistency of our results the yields of some selected isotopes of Co and Ni were compared with the previously measured data. The results were consistent within a factor of two, showing the stability and reproducibility of our laser ion source.

Production rates are summarized in table 1. For $^{68\text{-}74}$Ni and $^{67\text{-}70}$Co the production rates were taken from earlier studies [13]. As it was mentioned in [13], the global ion source efficiency was improved by a factor of 4.5 since the first measurements [6], thus, the already reported production rates were multiplied by this factor and added to the table. Due to the low-production rates of the $^{65\text{-}66}$Co isotopes, these rates were deduced from the number of detected β's. The laser ionization enhances the production of Co by about two orders of magnitude. Thus, one can deduce the production rate by subtracting the background β-counting rate (lasers off) from the on-

Table 1. Production rates (atoms/μC) of neutron-rich isotopes, produced in the 30 MeV proton-induced fission of ^{238}U. The numbers are corrected for the losses due to the delay time of the cell. The experimental uncertainties are given in brackets.

Mass number	Co	Ni	Cu	Ga
65	7 (3)			
66	10 (4)			
67	16 (5)			
68	11 (3)	16 (3)		
69	7 (3)	23 (4)		
70	1.3 (3)	28 (5)	12 (2)	
71		14 (3)	25 (7)	
72		5 (1)	65 (14)	
73		1.4 (3)	45 (10)	
74		0.20 (5)	21 (5)	5 (2)
75			8 (4)	33 (8)
76			2 (1)	76 (6)
77				119 (21)
78				102 (8)
79				79 (8)
80				26 (4)
81				9 (2)

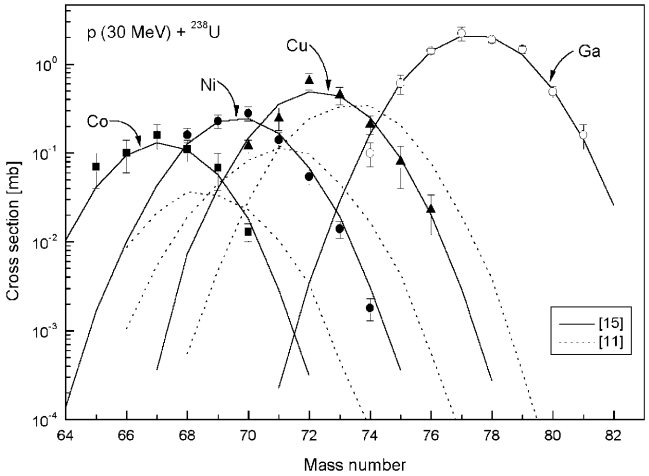

Fig. 1. The cross-section calculations ([15]: full line and [11]: dotted line) together with the scaled experimental production rates, corrected for the delay in the gas cell. For the data of Co, Ni and Cu a scaling factor of 0.01 mb $\cdot$ μC/atom was used. The gallium yields were obtained without laser ionization and were multiplied by 0.0182 mb $\cdot$ μC/atom. Note that because of the laser ionization it is possible to measure isotopic yields over a wide range of intensities.

Table 2. γ-ray energies that were used for the production rate evaluation. The absolute γ-ray intensity for the Cu isotopes and ^{75,77}Ga isotopes were taken from our studies, based on the γ-ray intensities of the daughter nuclide [17]. The intensities for the other Ga isotopes are taken from [17].

Cu			Ga		
	E (keV)	$I_{\rm abs}$ (%)		E (keV)	$I_{\rm abs}$ (%)
^{70}Cu	885	99(1)	^{74}Ga	596	91(1)
^{71}Cu	490	33(7)	^{75}Ga	252	29(3)
^{72}Cu	652	60(12)	^{76}Ga	563	66(5)
^{73}Cu	450	45(9)	^{77}Ga	469	20(4)
^{74}Cu	605	79(15)	^{78}Ga	620	77(4)
^{75}Cu	421	20(5)	^{79}Ga	465	24(1)
^{76}Cu	599	60(20)	^{80}Ga	659	79(8)
			^{81}Ga	217	37(2)

resonance β-counting rate and by correcting for the cumulative daughter activity. The production rates of the Ga isotopes were deduced from the number of detected γ-rays as well as β's. After correction for the daughter activity, isobaric and doubly charged isotope contamination (the latter information was available from the γ spectrum), both methods gave the same results within the experimental accuracy. The production rates of the Cu isotopes were determined by γ counting only.

The method of γ counting is based on the knowledge of the absolute γ-ray intensity. This information was available from [17]. Table 2 shows the γ-ray energies and their absolute intensities that were used. The deduction of production rates includes straightforward corrections for the implantation cycle and the isotope's half-life.

For very short-lived isotopes the evacuation time in the gas cell becomes important. This delay is a complex function of the gas cell parameters. From on-line measurements [18] one can deduce that an exponential function $e^{0.2/\tau}$ (mean delay time 200 ms) can be used to correct the production rates, where τ is the mean life of the isotope under study given in seconds. Some nuclei have high- and low-spin isomers (^{69}Ni, ^{68,70}Co). The high- to low-spin ratio was 6.1, 1.3 and 0.5 for ^{69}Ni, ^{68}Co and ^{70}Co, respectively. Corrections for the decay losses were taken into account. In table 1 and fig. 1 the total production rates (thus, the sum of the rates of the two isomers, where applicable) are given.

3 Comparison with cross-section calculations

3.1 The fission model PROFI

The fission model PROFI is a Monte Carlo code based on a semi-empirical approach to the fission process. In this model, the population of the fission channels is assumed to be basically determined by the statistical weight of transition states above the potential-energy landscape near the fission barrier. Several properties, however, are finally determined at scission. A full description of the model is given in ref. [14]. Some minor improvements were added to the model recently.

The barrier as a function of the mass asymmetry is defined by three components. The first is the component defined by the liquid-drop potential by means of a parabolic function with a curvature obtained from experimental data [19]. This parabola is assumed to be modulated by

two neutron shells, located at mass asymmetries corresponding to neutron numbers $N = 82$ (spherical neutron shell) and $N = 90$ (deformed neutron shell). We assume that the mass-asymmetric degree of freedom at the fission barrier is on average uniquely related to the neutron number of the fragments. The shells are represented by Gaussian functions. These shells are associated with the fission channels Standard I and Standard II, respectively, while the liquid-drop potential is associated with the symmetric fission channel. The population of the fission channels is proportional to the level density around the corresponding dips in the potential at saddle at a given excitation energy. Shells are supposed to wash out with excitation energy [20]. The heights and the widths of the Gaussians representing the shell effects and additional fluctuations in mass asymmetry acquired from saddle to scission are derived from experimental data [14]. The mean values of the neutron-to-proton ratio (*i.e.* the charge polarisation) for Standard I and Standard II are deduced from measured nuclide distributions after the electromagnetic-induced fission of ^{238}U [21]. The charge polarisation for the symmetric fission channel and the fluctuations in the neutron-to-proton ratio for all channels are also considered by describing the potential in this degree of freedom by a parabolic function. Assuming that the equilibration in this variable is fast compared to the saddle-to-scission time, this potential was calculated in the scission configuration. Since the shell effects of the nascent fragments at scission are not known experimentally, because they are strongly deformed on the average, only macroscopic properties are included in this calculation. Consequently, two fission pre-fragments are obtained, and their excitation energies are calculated from the excitation and deformation energy of the fissioning system at the scission point.

The PROFI model is incorporated into the larger nuclear-reaction code ABRABLA [22]. The compound-nucleus formation preceding the fission and the de-excitation of the formed fission pre-fragments via particle evaporation are conducted by the routines within the ABRABLA code.

3.2 Comparison with cross-section calculations

In order to compare the experimental production rates with the cross-section calculations, the efficiency of the ion source should also be known. The efficiency is a complex function of the gas cell parameters (see below) but it should be equal for the different elements (Co, Ni and Cu), which are laser ionized. A normalization factor for scaling the production rates (given in atoms/μC) to the cross-section (given in mb) of $0.01\,\mathrm{mb}\cdot\mu\mathrm{C/atom}$ was obtained by matching the data of the nickel isotopes to the calculated distribution of Benlliure *et al.* [14,15]. The same factor was applied for Co and Cu isotopes. In this way a cross-section of 1 mb corresponds to a production rate of 100 atoms/μC. Since the Ga isotopes were produced without laser ionization, their production curve required a different scale factor, which resulted in $0.0182\,\mathrm{mb}\cdot\mu\mathrm{C/atom}$. The agreement between theory [14,15] and experiment is good. The calculation predicts correctly the relative production rates of Cu and Co *vs.* Ni. In fact this points once more to the reliable operation of the laser ion source as the measurements of a specific element require appropriate laser settings and the different measurements were performed during different experimental campaigns. For comparison we add to the plot the calculation of Rubchenya *et al.* [7, 11] for the nickel, cobalt and copper data. Normalizing the data to the latter calculation results in a factor of $0.004\,\mathrm{mb}\cdot\mu\mathrm{C/atoms}$. The similarity of the two normalization factors indicate that the two calculations agree on the order of magnitude of the cross-section, however the curve of Rubchenya *et al.* is shifted further away from stability. In order to obtain a closer comparison, the experimental and calculated data were fitted with a Gaussian function. Benlliure *et al.* reproduces the mean and width of the distributions very well (see table 3). However, the mean masses from calculations of Rubchenya *et al.* are off by about 1.5 mass units from the experimental data. Note also that this difference increases when going to lighter elements. The overall good agreement with the calculation of Benlliure *et al.* for this reaction gives confidence for its predictive power to unknown regions of the nuclear chart. Extrapolating the calculated cross-sections towards ^{78}Ni gives a value in the picobarn region, which is about three orders of magnitude smaller compared to the prediction of [11] (2.8 nb).

From the normalization factor, we can deduce the global ion source efficiency. According to the calculations, 22% of the ^{70}Ni isotopes that are produced in the ^{238}U targets are recoiled in the 500 mbar argon gas. This gives a total ion source efficiency of 0.05% for isotopes of nickel, copper and cobalt (with laser ionization), and 0.02% for gallium (without laser ionization). Note that the selectivity —defined as the yield with lasers over the yield without lasers— was of the order of 100 for nickel, copper and cobalt. If we assume that the model of Benlliure *et al.* gives a correct prediction of the relative cross-section between nickel and gallium, we can conclude that the non-resonant ionization —or ion survival probability— for Ga is about 40 times higher compared to nickel, copper and cobalt. This chemical dependence of the overall efficiency of ion guide systems where no laser ionization is implemented indicates that cross-sections calculated from yields extracted from them should be dealt with caution. It also shows that the performances of gas catcher systems do depend on the chemical properties of the isotopes of interest.

3.3 Optimization of the ^{78}Ni production cross-section

In order to optimize the yields of the extreme neutron-rich isotopes along the $Z = 28$ line, different beam-target combinations and beam energies were calculated using the model of Benlliure *et al.* mentioned above. We have limited the calculation to beams of light particles (p, d, ^{4}He) and medium energy ($E < 50$ MeV) as they can be produced in copious amounts with the Louvain-la-Neuve cyclotron, and to long-lived fissile targets: ^{232}Th, ^{238}U, ^{244}Pu, ^{250}Cm. It is not clear at this moment if, from the

Table 3. A comparison of the parameters from a Gaussian fit through the experimental data and through the calculations [15] and [11]. The error bars are taken from the fit $y = A \times \exp\left[-\frac{(x-x_0)^2}{2\sigma^2}\right]$.

	Mean x_0 (mass units)				Width σ (mass units)		
	Experiment	Calc. [15]	Calc. [11]	Difference between [11] and [15]	Experiment	Calc. [15]	Calc. [11]
Co	66.9(1)	67.16(1)	68.56(3)	1.40(3)	1.4(1)	1.41(1)	1.53 (3)
Ni	69.5(1)	69.69(1)	71.00(4)	1.31(4)	1.44(4)	1.45(1)	1.56 (3)
Cu	72.3(1)	72.27(1)	73.37(1)	1.10(1)	1.39(8)	1.46(1)	1.51 (1)
Ga	77.5(1)	77.44(1)	–	–	1.48(5)	1.52(1)	–

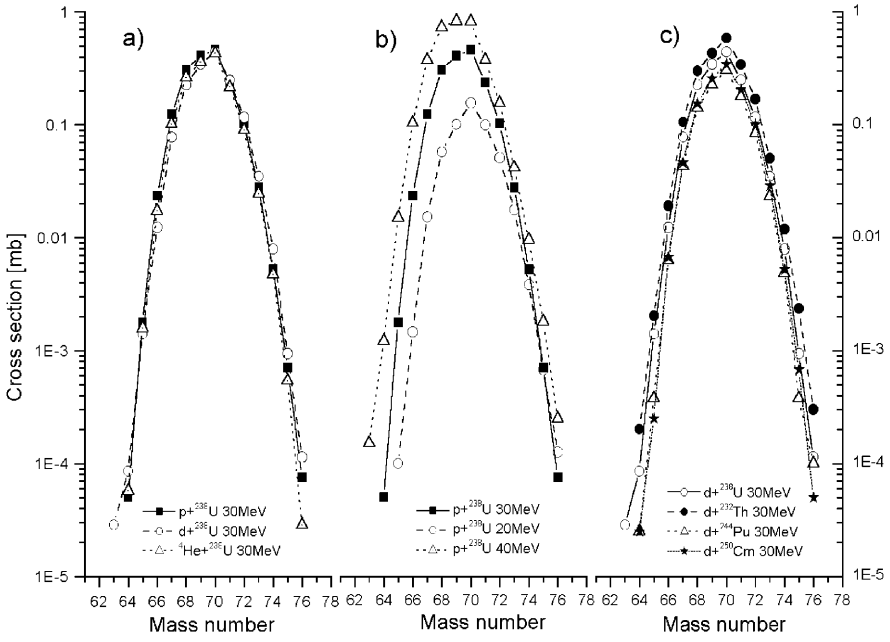

Fig. 2. Cross-section calculations using the PROFI code [15] for the production of Ni isotopes using a) different projectiles (p, d, ^{4}He) at 30 MeV on ^{238}U target; b) different projectile energies (20, 30, 40 MeV) for the reaction p + ^{238}U; c) deuterium particle at 30 MeV on different target materials (^{232}Th, ^{244}Pu, ^{250}Cm).

technical point of view, the latter two targets can be handled with the present laser ion source setup. The results obtained from the calculations are summarized in the following:

- Different beam particles:
  fig. 2a shows the results of the calculation of the cross-section of Ni ($Z = 28$) isotopes using p, d and ^{4}He beams of 30 MeV on ^{238}U target. The distributions are very close to each other and the difference for the very neutron-rich isotopes is minor.
- Different energies:
  the results for proton-induced fission on ^{238}U with particle energies from 20 to 40 MeV are shown in fig. 2b. Although the overall elemental production is greater for higher energies, the difference between the different energies becomes small for the heavier isotopes.
- Different targets:
  a comparison between the reactions with different targets and a deuterium beam of 30 MeV shows that the optimal case is ^{232}Th (d, fission). However, the gain for ^{76}Ni using this target over ^{238}U is only a factor of 2 to 3 (fig. 2c).

As a conclusion, according to these calculations the tested changes in beam, target and excitation energy did not improve the yields of heavy nickel isotopes in a significant way.

4 Conclusion

In this paper we report on yield measurements of neutron-rich cobalt, nickel, copper and gallium isotopes produced in the 30 MeV proton-induced fission of ^{238}U followed by thermalisation in a gas catcher and on-line mass separation. In the case of cobalt, nickel and copper resonant laser ionization has been applied to improve the efficiency and the selectivity. Because of this, the yields could be determined in a reliable way using γ as well as β counting. The data were compared with two cross-section calculations of which the one of Benlliure *et al.* reproduces the data well.

From this calculation the cross-section for the production of ^{78}Ni could be extracted to be of the order of a few picobarns, about three orders of magnitude lower compared to previous estimates. Different beam-target combinations and beam energies were also used in a separate calculation in order to optimize the cross-sections but they did not result in a substantial improvement for the most exotic nuclei. The global laser ion source efficiency for this fission reaction could be determined as 0.05% while the production of ions without laser ionization was about a factor of 100 lower for the isotopes of cobalt, nickel and copper. However for the gallium isotopes a 40 times higher ion survival probability was measured, indicating the influence of the physico-chemical properties of the elements of interest on the performances of the gas catcher systems.

In order to extend decay studies around ^{78}Ni, improvements in the performances of the laser ion source as well as in the detection systems have to be accomplished. A program to optimize the laser ion source based on careful off-line and on-line measurements is underway [23], while the development of efficient arrays of segmented germanium and silicon detectors is currently being pursued [24]. These developments will result in a major improvement of the sensitivity of the spectroscopy of nuclei in the vicinity of ^{78}Ni.

We would like to thank J. Gentens and P. Van den Bergh for technical assistance in operating the LISOL separator. The work is supported by the Inter-University Attraction Poles (IUAP) Research Program (Belgium), the Fund for Scientific Research-Flandrens, Belgium (FWO) and the Research Fund K.U. Leuven (GOA). K.V.d.V. is Research Assistant of the FWO-Vlaanderen.

References

1. W. Nazarewicz, J. Dobaczewski, T. Werner, Phys. Scr. T **56**, 9 (1995).
2. Ch. Engelmann *et al.*, Z. Phys. A **352**, 351 (1995).
3. K.-L. Kratz *et al.*, Z. Phys. A **340**, 419 (1991).
4. B. Ekstrom *et al.*, Phys. Scr. **34**, 614 (1986).
5. P. Armbruster *et al.*, Europhys. Lett. **4**, 793 (1987).
6. S. Franchoo *et al.*, Phys. Rev. Lett. **81**, 3100 (1998).
7. M. Huhta *et al.*, Phys. Lett. B **405**, 230 (1997).
8. O. Sorlin *et al.*, Nucl. Phys. A **669**, 351 (2000).
9. S. Czajkowski *et al.*, Z. Phys. A **348**, 267 (1994).
10. J.M. Daugas *et al.*, Phys. Lett. B **476**, 213 (2000).
11. V. Rubchenya, private communication.
12. Y. Kudryavtsev *et al.,* Nucl. Instrum. Methods B **114**, 350 (1996).
13. W. Mueller *et al.*, Phys. Rev. C **61**, 054308 (2000).
14. J. Benlliure *et al.*, Nucl. Phys. A **628**, 458 (1998).
15. J. Benlliure *et al.*, GSI Scientific Report GSI **2000-1**, 29 (1999).
16. L. Weissman *et al.*, Nucl. Instrum. Methods A **423**, 328 (1999).
17. R.B. Firestone, V.S. Shirley, *Table of Isotopes*, 8th edition (1996).
18. L.Weissman *et al.*, Nucl. Instrum. Methods A **483**, 581 (2002)
19. S.I. Mulgin *et al.*, Nucl. Phys. A **640**, 375 (1998).
20. A.V. Ignatyuk *et al.*, Sov. J. Nucl. Phys. **21**, 255 (1979).
21. T. Enqvist *et al.*, Nucl. Phys. A **658**, 47 (1999).
22. J.-J. Gaimard, K.-H. Schmidt, Nucl. Phys. A **531**, 709 (1991).
23. Y. Kudryavtsev *et al.*, Nucl. Instrum. Methods B **179**, 412 (2001).
24. D. Habs *et al.*, Progr. Part. Nucl. Phys. **38**, 111 (1997).